Journal of Controlled Release 155 (2011) 386–392

Contents lists available at ScienceDirect

Journal of Controlled Release

journal homepage: www.elsevier.com/locate/jconrel

Receptor-mediated activation of a proinsulin-transferrin fusion protein in hepatoma cells

Yan Wang, Yu-Sheng Chen, Jennica L. Zaro, Wei-Chiang Shen *

Department of Pharmacology and Pharmaceutical Sciences, University of Southern California, 1985 Zonal Ave, Los Angeles, CA 90033, United States

ARTICLE INFO

Article history:
Received 3 April 2011
Accepted 18 June 2011
Available online 2 July 2011

Keywords:
Proinsulin
Transferrin
Insulin
Prohormone conversion
Receptor-mediated endocytosis and recycling
Bifunctional fusion protein

ABSTRACT

A proinsulin-transferrin (ProINS-Tf) recombinant fusion protein was designed and characterized for the sustained release of an active form of insulin (INS) by hepatoma cells. During incubation with H4IIE hepatoma cells, a gradual decline of ProINS-Tf concentration, with a concomitant generation of the immuno-reactive insulin-transferrin (irINS-Tf), was detected in the culture medium by using INS- or proinsulin (ProINS)-specific radioimmunoassay (RIA) system. Further studies indicated that the conversion of ProINS-Tf to irINS-Tf was a transferrin receptor (TfR) mediated process that was pH-sensitive, and temperature- and microtubule-dependent. These results suggest that the conversion occurred during the slow recycling route of transferrin (Tf)-TfR pathway, possibly processed by proteases in the slow recycling compartments juxtaposed to the trans-Golgi network (TGN). ProINS-Tf exhibited little activity in the short-term promotion of glucose uptake in adipocytes, indicating that it was in an inactive form similar to ProINS. Stimulation of Akt phosphorylation by ProINS-Tf was detected only after prolonged incubation with H4IIE cells. On the other hand, ProINS-Tf pre-incubated with H4IIE cells for 24 h acquired an immediate activity of stimulating Akt phosphorylation. Furthermore, ProINS-Tf elicited a strong activity in the inhibition of glucose production following 24 h incubation with H4IIE cells. Based on these findings, we conclude that the Tf–TfR endocytosis and recycling pathway enables the conversion and release of ProINS-Tf in an active form of irINS-Tf. Results from this study suggest that the Tf–TfR pathway can be exploited for the design of prohormone-Tf fusion proteins as protein prodrugs for their sustained and targeted activation.

© 2011 Elsevier B.V. All rights reserved.

1. Introduction

The therapeutic potential of ProINS, the single-chain precursor to INS, has been evaluated in both preclinical and clinical studies [1]. ProINS was marginally hepatospecific, having greater effects on hepatic glucose production than peripheral glucose disposal [2]. Additionally, pharmacokinetic studies demonstrated that both the distribution and the elimination half-life of ProINS were longer than INS [3]. Despite these potential advantages, the application of ProINS faces formidable challenges due to the low potency of ProINS (4 U/mg for ProINS in contrast to 28 U/mg for INS [1]) and the low *in vivo* conversion of ProINS to INS [4,5]. High doses are consequently required for ProINS to achieve *in vivo* pharmacological efficacy. Results from the ProINS clinical trials also showed an increased risk for myocardial infarction, and further clinical studies were subsequently suspended due to safety concerns [1].

The aims of this study were to utilize Tf-fusion protein technology to overcome some of the challenges encountered in the development of ProINS as a hypoglycemic agent. Human Tf is a circulatory serum protein responsible for iron transport, and there are numerous reports on the application of Tf as a fusion protein either to facilitate oral absorption of protein drugs, such as granulocyte-colony stimulating factor-Tf and human growth hormone-Tf fusion proteins [6,7], or to prolong plasma half-life of protein drugs, such as glucagon-like peptide-1-Tf fusion protein [8]. However, another unexploited advantage of Tf-fusion protein technology is the endocytosis and recycling mechanisms of the Tf–TfR pathway. After binding and subsequent receptor-mediated endocytosis of the Tf–TfR complex, Tf unloads iron in the acidic endosomal compartments. Iron-free Tf (apo-Tf) remains bound to TfR intracellularly and is recycled back to the cell surface for release [9,10]. Tf can be delivered to intracellular compartments such as the TGN [11]. Many studies observed the merging of endocytosed Tf with the protein secretory pathway in vesicles located at the TGN [12,13], which conceivably would allow access of endocytosed Tf to secretory proteases that are responsible for the conversion and activation of prohormones. A distinctive feature of Tf is that, unlike most ligands that are sorted to the lysosome for degradation, it is released at the cell surface intact. To our knowledge, this final release step of Tf from TfR following recycling has not been taken advantage of in the development of Tf-fusion proteins.

* Corresponding author at: 1985 Zonal Avenue, PSC 404B, Los Angeles, CA 90033, United States. Tel.: +1 323 442 1902; fax: +1 323 442 1390.
E-mail address: weishen@usc.edu (W.-C. Shen).

0168-3659/$ – see front matter © 2011 Elsevier B.V. All rights reserved.
doi:10.1016/j.jconrel.2011.06.029

In this report, we describe the design and characterization of a ProINS-Tf fusion protein. Our results showed that ProINS-Tf was converted to an active form of INS by hepatoma cells. Furthermore, we demonstrated that the conversion and activation of ProINS-Tf is a TfR-mediated process, occurring inside the recycling compartments along the Tf–TfR pathway. To the best of our knowledge, this is the first report indicating that a ProINS fusion protein can be delivered as a prodrug to be processed and activated by hepatoma cells under the control of the Tf–TfR endocytic and recycling pathway.

2. Materials and methods

2.1. Construction and production of his-tagged ProINS-Tf recombinant fusion protein

A Gly-Gly-Ser-hexa His sequence (–GGSHHHHHH–) was incorporated into the carboxyl-terminal region of the full-length human Tf (residues 1–679) to make a his-tagged Tf (Tf-$GGSH_6$) using PCR-based mutagenesis methods. TFR27 plasmid (ATCC, Manassas, VA) containing the full-length human Tf sequence (NM_001063) was used as PCR templates. The mutagenic forward and reverse primers were designed as 5 -CCGCTCGAGGTCCCTGATAAAACTGTGAGATGGT-3 and 5 -TGCTCTAGACTA**ATGATGATGATGATGATG***GCTGCCCCC*AGGTCTACG-GAAAGTGcaggcttcc-3 (the hexa His sequence is indicated in bold print, and the Gly-Gly-Ser sequence is indicated in italics). The cDNA sequence coding for preproinsulin (NM_000207) was amplified from commercial plasmid (SC120054, Origene, Rockville, MD). Preproinsulin sequence fused upstream in frame with Tf-$GGSH_6$ sequence was subsequently engineered into pcDNA3.1 (+) expression vector (Invitrogen, Carlsbad, CA) through EcoRV, XhoI, and XbaI restriction enzymes sites. A leucyl-glutamyl dipeptide sequence was incorporated between ProINS and Tf due to the XhoI restriction enzyme recognition site.

The plasmids containing preproinsulin-Tf-$GGSH_6$ fusion gene were transiently transfected to HEK293 cells through polyethylenimine-mediated DNA transfection. Conditioned serum-free CD 293 medium (Invitrogen) was collected twice every 4 days, and concentrated using a tangential flow filtration system (Millipore, Billerica, MA). The concentrates were then applied to Ni-NTA column (Qiagen, Valencia, CA) to allow binding of his-tagged ProINS-Tf to Ni-NTA agarose. After washing with 20 mM imidazole to remove the impurities, his-tagged ProINS-Tf was eluted from the column using 250 mM imidazole. The excess imidazole was removed by overnight dialysis using Spectra/Por dialysis membrane (MWCO 12–14 kDa, Spectrum Laboratory, Rancho Dominguez, CA) against phosphate buffer containing 50 mg/mL mannitol and 0.1 mg/mL Tween-20. The purified ProINS-Tf fusion protein was quantified by resolving in 8% non-reducing SDS-PAGE followed by both Coomassie blue staining and Western blot against anti-Tf antibody (T2027, Sigma, St. Louis, MO) and anti-(Pro)INS antibody (INS+ProINS antibody, ab8304, Abcam, Cambridge, MA).

2.2. ProINS- and INS-specific RIA

Cultured H4IIE rat hepatoma cells (ATCC) were treated with ProINS-Tf, in the presence or absence of a 1000-fold excess of apo-Tf (Sigma) or BSA (Sigma). To measure the remaining concentration of ProINS-Tf in the cultured medium, media were collected after different incubation time-points, and subjected to human ProINS-specific RIA (Millipore) according to the manufacturer's instructions. The ProINS-specific RIA has less than 0.1% cross-reactivity with human INS. On the other hand, to quantify the generated irINS-Tf, cell culture media were collected at different incubation time-points, and applied to human INS-specific RIA (Millipore) that has less than 0.2% cross-reactivity with human ProINS. In order to evaluate the cell membrane integrity following the treatment conditions, cells treated with ProINS-Tf, in the presence or absence of excess apo-Tf or BSA for 24 h were analyzed by the lactate dehydrogenase (LDH) release assay (Promega, Madison, WI) according to the manufacturer's instructions.

2.3. 2-Deoxyglucose uptake in cultured adipocytes

3T3-L1 murine fibroblasts (ATCC) were differentiated into adipocytes as previously described [14]. Adipocytes were serum-starved in DMEM containing 0.5% BSA for 16 h before experiments. Cell monolayers were incubated with different concentrations of INS (Sigma), ProINS (R&D System, Minneapolis, MN), or ProINS-Tf in Krebs–Ringer phosphate buffer supplemented with 0.1% BSA for 30 min at 37 °C. After 30 min, 0.5 μCi/mL of 2-deoxy-D-[2, 6-^{3}H] glucose (Perkin Elmer, Waltham, MA) was added to the cells and incubated for 10 min. The reaction was stopped by aspirating the medium, and the cells were washed four times with ice-cold Krebs–Ringer phosphate buffer. Cells were then solubilized with 0.1 M NaOH/0.1% sodium dodecyl sulfate, followed by measurement of the internalized 2-deoxy-D-[2, 6-^{3}H] glucose using a scintillation counter (Perkin Elmer) and protein quantification using the bicinchoninic acid (BCA) assay (Thermo Fisher Scientific, Rockford, IL).

2.4. Measurement of Akt phosphorylation

Upon binding of INS to insulin receptor (IR), Akt is phosphorylated following activation of the PI 3-kinase signaling pathway [15]. Quiescent H4IIE cells (~18 h serum-starved) were treated with or without proteins in serum-free conditions. After treatment, cells were immediately lysed with cell extraction buffer (Invitrogen) supplemented with phenylmethanesulfonyl fluoride (Sigma) and protease inhibitor cocktail (Sigma). After protein quantification, an equal amount of cellular proteins (60 μg) was subjected to Western blot analysis by anti-phospho-Akt antibody (Ser 473, 4060, Cell Signaling Technology, Danvers, MA) and anti-beta-actin antibody (AC-15, A5441, Sigma). Immunoreactive bands were detected using enhanced chemiluminescence (GE Health care, Piscataway, NJ), and quantified using Quantity One 1-D Analysis software (Bio-Rad, Hercules, CA).

2.5. Glucose production assay in H4IIE cells

Glucose production was determined using a modified method from previous reports [16]. H4IIE cells were grown in 24-well plates in high-glucose DMEM containing 10% FBS. Serial dilutions of human ProINS, human INS, or ProINS-Tf fusion protein were prepared in serum-free DMEM. Upon confluence, cells were washed with PBS twice to remove excess serum, and treated with various concentrations of proteins for 24 h at 37 °C. Cells were then incubated for 3 h in glucose production medium consisting of serum-, glucose- and phenol red-free DMEM supplemented with 2 mM sodium pyruvate and 40 mM sodium DL-lactate. The medium was harvested and glucose concentrations were measured using the Amplex Red Glucose/Glucose Oxidase Kit (Invitrogen). Cellular protein was quantified using the BCA assay.

2.6. Statistical analysis

The data are presented as average plus standard deviation with $N = 3$ for all experiments. The Student's *t*-test was utilized to compare data sets, where differences with values of $p < 0.05$ were considered statistically significant.

3. Results

3.1. Expression and characterization of ProINS-Tf recombinant fusion protein

Human preproinsulin was ligated in frame with carboxyl-terminally his-tagged Tf into pcDNA3.1 vector. Preproinsulin-Tf-$GGSH_6$ fusion gene

was transfected to HEK293 cells to express recombinant his-tagged ProINS-Tf fusion protein, during which the N-terminal signal peptide of preproinsulin was cleaved in the endoplasmic reticulum (Fig. 1A). The Coomassie blue staining (Fig. 1B) and Western blots against both anti-Tf and anti-(Pro)INS (Fig. 1C) demonstrated one major band corresponding the molecular weight of the ProINS-Tf fusion protein (~89 kDa), which indicated that ProINS-Tf was expressed and secreted into media. The lack of free Tf observed on anti-Tf blot indicated that the dipeptide linker incorporated between ProINS and Tf remained stable during the protein production process. A minor band was present between 130 kDa and 250 kDa on the anti-Tf blot, which was possibly a dimerized fusion protein (~180 kDa). This band was not visible on the anti-(Pro)INS blot, presumably due to the low detection limit of the anti-(Pro)INS antibody.

3.2. ProINS-Tf was converted to irINS-Tf through Tf–TfR mediated slow recycling pathway during incubation with H4IIE hepatoma cells

The ProINS-specific RIA with less than 0.1% cross-reactivity to human INS was used to detect ProINS-Tf concentration after incubating with H4IIE cells for different time intervals. When 100 pM of ProINS-Tf was incubated with H4IIE cells, only 19% of the fusion protein was detected in the cell-treatment medium after 24 h. However, when incubated in cell-free medium, the concentration of ProINS-Tf remained relatively stable. The loss of ProINS-Tf during H4IIE cell incubation was significantly blocked in the presence of excess apo-Tf, resulting in 91% remaining detectable after 12 h and 61% after 24 h. In contrast, adding excess BSA had no significant effect on the ProINS-Tf detectable concentration (Fig. 2A). None of the treatments caused leakage of LDH at the 24 h time-point compared to the non-treated group, indicating that cell membrane integrity was maintained during the treatments (Fig. 2B).

An INS-specific RIA with less than 0.2% cross-reactivity to human ProINS was also used to determine whether the loss of ProINS-Tf correlated with a generation of irINS-Tf after incubation with H4IIE cells. Starting after 2 h of incubation, irINS-Tf was detected and gradually accumulated in cell-treatment medium until 24 h of incubation. Similar to the loss of detectable ProINS-Tf, the generation of irINS-Tf was almost completely inhibited in the presence of excess apo-Tf, but not excess BSA (Fig. 3A). In contrast to ProINS-Tf, ProINS was not converted to irINS by H4IIE cells during the 24-h incubation

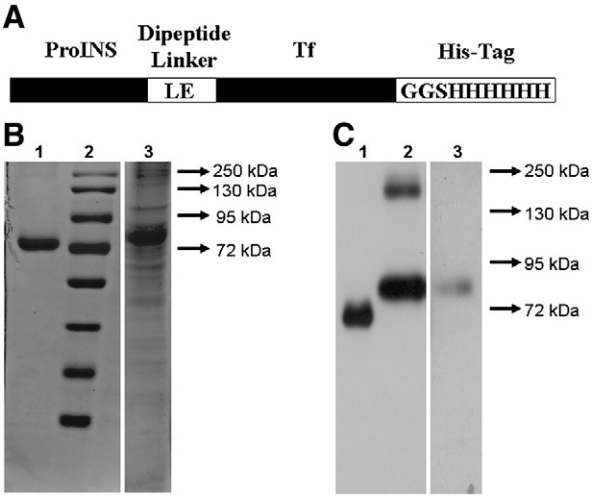


Fig. 1. Design and production of ProINS-Tf recombinant fusion protein. (A) Domain structure of his-tagged ProINS-Tf fusion protein. (B and C) After purification and concentration, protein samples were resolved in 8% non-reducing SDS-PAGE, followed by Coomassie blue staining (B) and Western blot with antibodies (C). For (B) Lane 1: human apo-Tf. Lane 2: marker. Lane 3: ProINS-Tf fusion protein. For (C), Lane 1: human apo-Tf in anti-Tf blot. Lane 2: ProINS-Tf fusion protein in anti-Tf blot. Lane 3: ProINS-Tf fusion protein in anti-(Pro)INS blot.

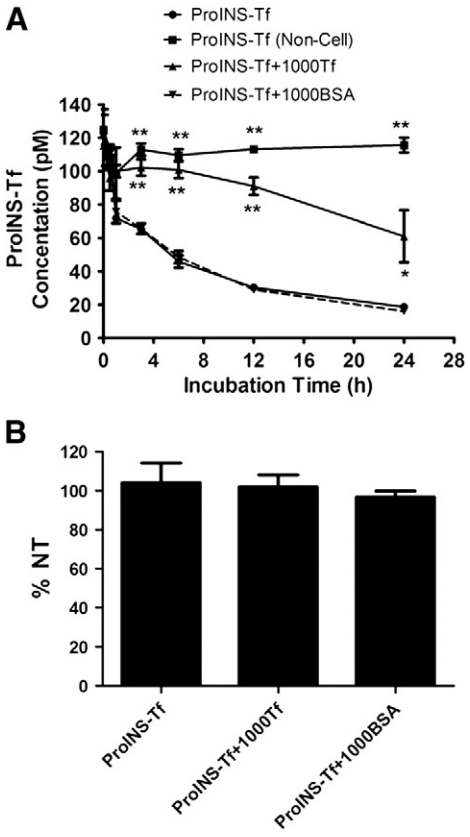


Fig. 2. Progressive decrease of ProINS-Tf fusion protein in H4IIE cells. (A) ProINS-Tf (100 pM), in the presence or absence of a 1000-fold excess of apo-Tf or BSA (ProINS-Tf + 1000Tf or ProINS-Tf + 1000BSA, respectively), were incubated either with H4IIE cell monolayers or in blank wells (non-cell) at 37 °C. Media were collected at different time-points and subject to ProINS-specific RIA to quantify ProINS-Tf fusion protein. The concentration of ProINS-Tf was calculated based on a standard curve of ProINS-Tf (ranging from 10 pM to 300 pM) according to the manufacturer's instructions. Data obtained from three treatment groups were shown as averages, with error bars indicating the standard deviation (N = 3). Data were marked with an asterisk (*) to indicate statistically significant differences compared to ProINS-Tf using the Student's *t*-test (*$p<0.05$, **$p<0.01$). (B) Membrane integrity remained intact after treating H4IIE cells with ProINS-Tf alone, or in the presence of excess apo-Tf or BSA. Levels of released LDH were measured and normalized to non-treated (NT) groups. All data were expressed as average, with error bars indicating the standard deviation (N = 3).

(Fig. 3A). The cell-treatment media after 24 h incubation of 10 nM ProINS-Tf with H4IIE cells was also analyzed by anti-Tf Western blot. The lanes containing the cell-treatment media at two different loading volumes showed a single band corresponding to the molecular weight of the fusion protein, while bands corresponding to free Tf were not detected (Fig. 3B).

The role of TfR-mediated endocytosis and/or recycling in irINS-Tf generation was further evaluated by altering the intracellular protein trafficking and processing. Fig. 3C demonstrated that the conversion of ProINS-Tf to irINS-Tf by H4IIE cells was temperature-dependent, as incubating the cells at 16 °C almost completely abolished the conversion. On the other hand, compared to the non-treated control, 86.4% and 83.0% of the irINS-Tf conversion were inhibited when ProINS-Tf was co-incubated for 8 h with the lysosomotropic agents ammonium chloride (20 mM) and chloroquine (50 μM), respectively. Additionally, co-incubating ProINS-Tf with a microtubule-disrupting reagent nocozadole (80 μM) blocked 50.9% of the conversion (Fig. 3D).

3.3. ProINS-Tf was inactive in short-term promotion of glucose uptake in cultured adipocytes

ProINS-Tf fusion protein was evaluated for the *in vitro* activity in promoting glucose uptake in cultured adipocytes. Compared to non-

treated control, INS exhibited ~6-fold and ~9-fold of glucose uptake at 10 nM and 100 nM, respectively. However, the proprotein ProINS showed considerably less activity with only ~1.3-fold (10 nM) and ~4.3-fold (100 nM) of glucose uptake compared to non-treated control. The activity of ProINS-Tf fusion protein was minimal with only ~1.2-fold of glucose uptake at both 10 nM and 100 nM (Fig. 4). Therefore, ProINS-Tf was considered inactive in the promotion of glucose uptake in adipocytes.

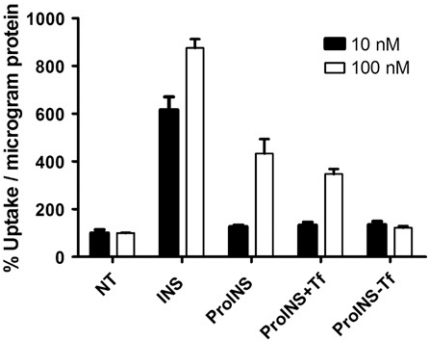


Fig. 4. ProINS-Tf was inactive in short-term promotion of glucose uptake in adipocytes. 3T3-L1 cells were induced to differentiate into adipocytes as described in the Materials and methods section. After treating cells with 10 nM or 100 nM of different proteins [INS, ProINS, ProINS-Tf, or equimolar mixture of ProINS and Tf (indicated as "ProINS + Tf")] for 30 min at 37 °C, 2-deoxy-D-[2, 6-^{3}H] glucose was added to the dosing solutions for another 10 min incubation. Cells were washed with ice-cold Krebs–Ringer phosphate buffer and dissolved in 0.1 M NaOH/0.1% sodium dodecyl sulfate. Cell lysates, mixed with scintillation fluid, were analyzed by a beta-counter to measure radioactivity. Results were calculated as cpm normalized by protein quantification. Data were expressed as the average percentage of uptake compared to NT groups, with error bars indicating the standard deviation (N = 3).

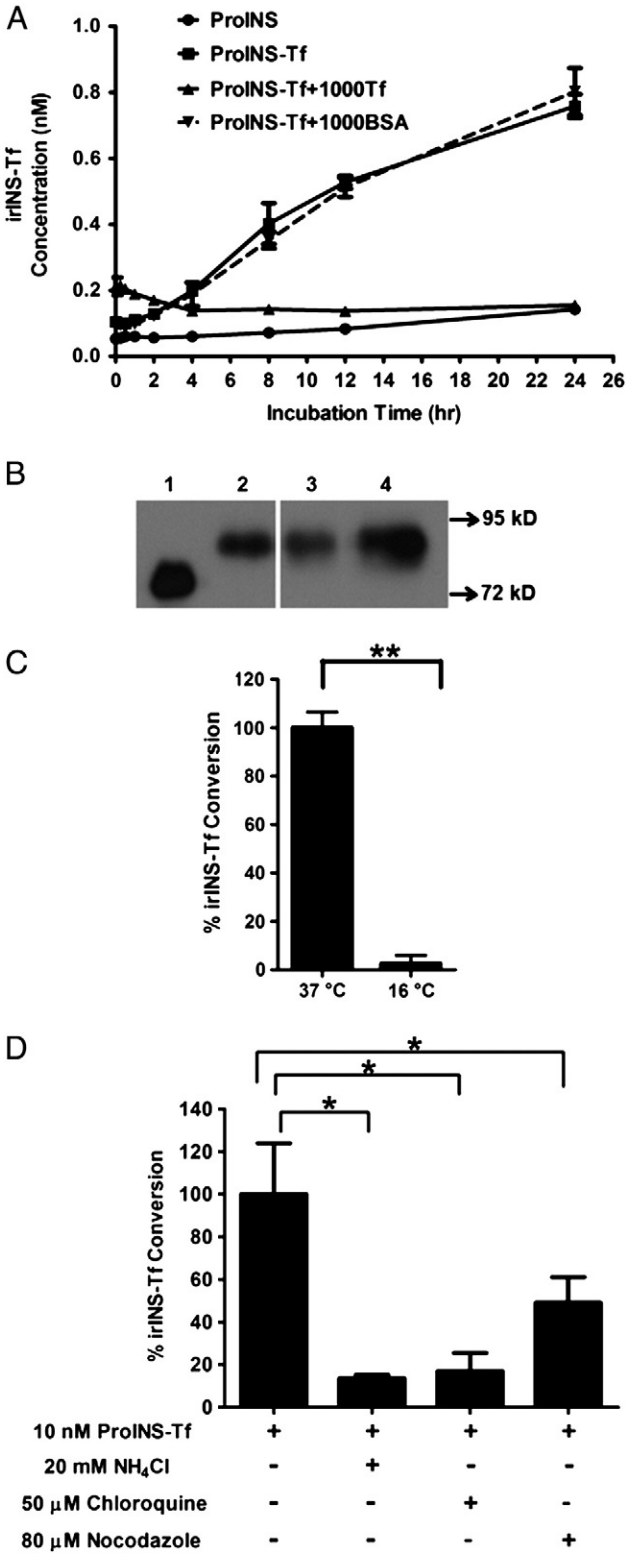


Fig. 3. Conversion of ProINS-Tf to irINS-Tf in H4IIE cells. (A) H4IIE cells were treated with 10 nM of ProINS, or 10 nM of ProINS-Tf in the presence or absence of 1000-fold excess of apo-Tf or BSA at 37 °C (ProINS-Tf + 1000Tf or ProINS-Tf + 1000BSA, respectively). At the indicated time-points, media were collected and analyzed using INS-specific RIA to detect the amount of irINS-Tf. The concentration of irINS-Tf was determined against a standard curve of human INS (ranging from 12 pM to 1200 pM) according to the manufacturer's instructions. (B) ProINS-Tf fusion protein (10 nM) was incubated in H4IIE cells for 24 h. Media were collected and centrifuged, and the supernatants were subject to 8% non-reducing SDS-PAGE, followed by immunoblotting with anti-Tf antibody. Lane 1: human Tf (20.0 ng, 5 μL). Lane 2: ProINS-Tf fusion protein (13.4 ng, 15 μL). Lane 3: H4IIE-treated media (15 μL). Lane 4: H4IIE-treated media (30 μL). (C) ProINS-Tf fusion protein (10 nM) was incubated with H4IIE cells for 12 h at 37 °C or 16 °C. The conversion of irINS-Tf was quantified using INS-specific RIA, and the data represented the average percentage of irINS-Tf conversion at 16 °C compared to the conversion at 37 °C. (D) ProINS-Tf fusion protein (10 nM) was incubated in the absence or presence of 20 mM ammonium chloride, 50 μM chloroquine, or 80 μM nocodazole at 37 °C for 8 h. The amount of converted irINS-Tf in different treatment groups was analyzed using INS-specific RIA. Data were expressed as the average percentage of irINS-Tf conversion compared to ProINS-Tf groups. For (C) and (D), * indicated $p<0.05$, ** indicated $p<0.01$ as determined by the Student's t-test (N = 3).

3.4. ProINS-Tf elicited activated Akt signaling during incubation with H4IIE hepatoma cells

In order to test whether the converted irINS-Tf would elicit active INS signaling, the kinetic changes of Akt phosphorylation stimulated by ProINS-Tf in H4IIE cells were investigated and also compared to that stimulated by INS or ProINS. Fig. 5A showed that INS exhibited a rapid onset with phospho-Akt reaching the maximal level after 5 min of incubation, and it subsequently decreased in a time-dependent manner until 24 h. Conversely, ProINS showed very little effect after 5 min of incubation. Although stimulation of Akt phosphorylation by ProINS slightly increased after 24 h, it was nevertheless considerably lower than that by INS. In contrast to both INS and ProINS, ProINS-Tf elicited distinct kinetic patterns of Akt phosphorylation. For ProINS-Tf-treated cells, Akt phosphorylation was at a very low level after the 5 min short-term incubation, which was similar to the ProINS-treated cells. However, Akt phosphorylation considerably increased after 4 h and sustained until 24 h of incubation.

In order to further evaluate the activation of ProINS-Tf over the 24 h incubation, ProINS-Tf or ProINS was first pre-incubated with H4IIE cell monolayers for 24 h, and then applied to fresh, quiescent H4IIE cells for the 5 min short-term incubation. Compared with ProINS-Tf pretreated in blank wells, H4IIE-pretreated ProINS-Tf

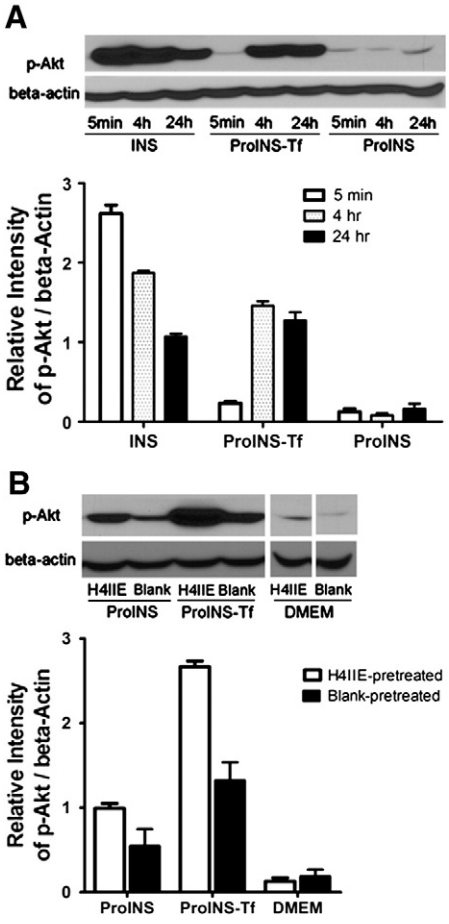


Fig. 5. ProINS-Tf exhibited activated stimulation of Akt phosphorylation during prolonged incubation with H4IIE cells. (A) H4IIE cells, deprived from serum overnight (~18 h), were treated with 100 pM of INS, ProINS, or ProINS-Tf at 37 °C for 5 min, 4 h, and 24 h, respectively. After cell lysis in the presence of protease and phosphatase inhibitors, 60 μg of total protein was subjected to 10% SDS-PAGE and immunoblotted against phospho-Akt and beta-actin antibodies. (B) DMEM, 1.1 nM ProINS or 1.1 nM ProINS-Tf were pre-incubated either with H4IIE cell monolayers or in blank wells. After 24 h, the incubation media were collected, centrifuged and applied to serum-starved H4IIE cells again for a 5 min short-term incubation. Subsequently, cells were lysed and cellular phospho-Akt and beta-actin levels were measured. Relative signal intensities were quantified by densitometry, and data were expressed as the average of relative intensity, with error bars indicating the standard deviation (N = 3).

elicited a significantly increased Akt phosphorylation. However, no significant increase was observed for either H4IIE-pretreated ProINS or H4IIE-pretreated DMEM, compared with the respective blank-pretreatment controls (Fig. 5B).

3.5. Enhanced activity of ProINS-Tf in inhibiting glucose production in H4IIE hepatoma cells

The inhibitory effect of ProINS-Tf in glucose production was determined following 24 h incubation with H4IIE hepatoma cells. ProINS-Tf fusion protein ($IC_{50} = 52.1 \pm 8.5$ pM) exerted a ~24-fold and ~6-fold stronger activity compared with ProINS ($IC_{50} = 1291.3 \pm 148.5$ pM) and INS ($IC_{50} = 308.9 \pm 19.7$ pM), respectively (Table 1). The inhibitory activity of an equimolar mixture of ProINS and Tf did not increase compared to ProINS. On the other hand, co-incubation of ProINS-Tf with 1000-fold excess of apo-Tf resulted in a significant reduction of the increased activity of ProINS-Tf, whereas co-incubating ProINS-Tf with 1000-fold excess of BSA did not increase the IC_{50} of ProINS-Tf (Fig. 6 and Table 1).

Table 1
The IC_{50} values of different proteins in the inhibition of glucose production in H4IIE cells.

Protein	IC_{50} (pM)[a]
INS	308.9 ± 19.7[b]
ProINS	1291.3 ± 148.5[c]
ProINS + Tf (equimolar)	1428.5 ± 677.3[b]
ProINS-Tf	52.1 ± 8.48
ProINS-Tf + 1000Tf	>1000
ProINS-Tf + 1000BSA	33.6 ± 6.13[b]

[a]Data represent averages ± standard deviation (N = 3).
[b]Indicated $p<0.05$ and [c] indicated $p<0.01$, compared to ProINS-Tf, as determined by the Student's *t*-test.

4. Discussion

In the present study, we employed a Tf-based fusion protein strategy combined with his-tag technology to produce a purified ProINS-Tf fusion protein. ProINS was designed upstream of Tf to allow better folding of ProINS. Since previous studies of the crystal structure of Tf indicated that the carboxyl-terminal three residues were buried in the interior of the Tf C-lobe [17], a tripeptide linker –GGS– was inserted between Tf and the his-tag sequence in order to make the his-tag accessible to the metal chelate column for purification. The his-tag was not designed to be cleaved after purification because it has been shown that the presence of a carboxyl-terminal his-tag does not interfere with the binding ability of Tf to TfR [18].

After incubating ProINS-Tf with H4IIE cells, we observed a progressive generation of irINS-Tf, along with a decline of detection for the proprotein form in culture media (Figs. 2 and 3A). ProINS-Tf had minimal irINS-containing components at the initial time of incubation, which implied that ProINS-Tf did not undergo significant conversion to irINS-Tf during production in HEK293 cells. In addition, both the conversion of ProINS-Tf to irINS-Tf (Fig. 3) and the inhibition of glucose production in H4IIE cells (Table 1 and Fig. 6) were decreased in the presence of excess apo-Tf, while neither the conversion nor the bioactivity was reduced in the presence of excess BSA. A slight decrease in the IC_{50} of ProINS-Tf in the presence of BSA was noted. This may result from the general effect of BSA in the protection of proteins from non-specific protease degradation [19]. However, this effect is considered minimal, since the change in IC_{50} values was small (Table 1 and Fig. 6), and since no significant increase in conversion to irINS-Tf was noted in the presence of BSA (Fig. 3A).

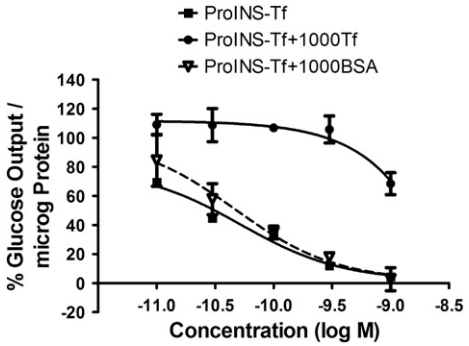
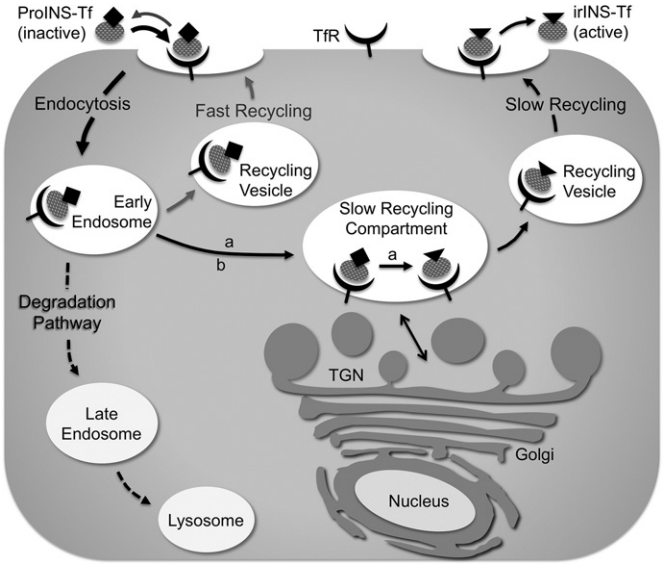


Fig. 6. Increased inhibition of glucose production by ProINS-Tf in H4IIE cells is mediated through Tf. Upon confluence, H4IIE cells were treated with various concentrations of ProINS-Tf fusion protein for 24 h. To detect the blocking effects of excess apo-Tf or BSA, cells were first pretreated with 1000-fold excess of apo-Tf or BSA for 30 min to pre-occupy the surface receptors, followed by the 24 h co-treatment of ProINS-Tf with 1000-fold excess of apo-Tf or BSA ("ProINS-Tf + 1000Tf" or "ProINS-Tf + 1000BSA"). Following incubation, the glucose output measurement was performed as described in the Materials and methods section. All data were expressed as average glucose levels normalized after protein quantification, with error bars indicating the standard deviation (N = 3).



Scheme 1. A hypothetical model of ProINS-Tf conversion to irINS-Tf in hepatoma cells. Following TfR binding on the cell membrane, ProINS-Tf/TfR complex is endocytosed to the early endosome. ProINS-Tf undergoes TfR-mediated recycling pathway, instead of being sorted to the late endosome and lysosome for degradation like many protein-receptor complexes. During the fast recycling, ProINS-Tf is rapidly recycled and released as an intact protein. During the slow recycling, ProINS-Tf is delivered to the slow recycling compartments that merge with vesicles from protein secretory pathway at the TGN, giving access of ProINS-Tf to secretory proteases that can convert ProINS-Tf to irINS-Tf. The generated irINS-Tf is subsequently recycled and released into the culture media. Reduced conversion efficiency was observed following treatment (a) with lysosomotropic agents, which inhibit vesicular fusion of the slow recycling pathway and inactivate pH-sensitive proteases, and (b) with the microtubule-disrupting agent nocodazole or incubation at 16 °C, which both inhibit the slow recycling pathway.

Based on our results, we believe that ProINS-Tf is converted to irINS-Tf utilizing the Tf–TfR pathway (Scheme 1). The binding affinity of ProINS to IR, which is also expressed in H4IIE cells [20], is about two orders of magnitude lower than that of Tf to TfR [10,21]. Thus the endocytosis of ProINS-Tf should be predominantly directed through the Tf–TfR, rather than the INS-IR pathway. Furthermore, the conversion did not result from non-specific degradation by proteases on plasma membranes or inside the cells, but rather from processing by certain convertases in TfR-associated intracellular compartments. These hypotheses illustrated in Scheme 1 are supported by our results showing that (a) both the decline of ProINS-Tf and the increase in irINS-Tf were inhibited in the presence of excess Tf (Figs. 2 and 3A), (b) ProINS was not converted to irINS following incubation (Fig. 3A), and (c) several known reagents that inhibit the Tf–TfR intracellular endocytic processing events (e.g., incubation at 16 °C, or in the presence of ammonium chloride, chloroquine, or nocodazole) resulted in a drastic inhibition in the conversion of ProINS-Tf to irINS-Tf (Fig. 3B, C, and D). In addition, results of LDH release assay, which is an indicator of membrane integrity [22,23], suggested that ProINS-Tf fusion proteins did not cause cell membrane destruction to release non-specific cytosolic proteases to the cell surface.

It is well accepted that two different Tf–TfR recycling routes exist. One is a fast recycling route through early endosomes, where the majority of internalized Tf is found to be recycled through this route within 10 min after endocytosis. The other is a slow recycling route (usually takes >30 min) through recycling compartments that are biochemically distinct from early endosomes and are usually found at a perinuclear region near the TGN [11,24]. Many reports of TfR trafficking demonstrated that TfR was delivered to the TGN as a part of the normal course of its intracellular sorting [11]. Our evidence also indicated that the conversion of ProINS-Tf to irINS-Tf most likely occurred during the slow recycling rather than the fast recycling route. First, the generated irINS-Tf was not detected until after incubation for 2 h (Fig. 3A), which was longer than expected for the fast recycling route. Second, the conversion was significantly reduced in the presence of lysosomotropic agents, which inhibit vesicular compartment fusion events that primarily occur in the slow recycling pathway. Third, the temperature- and microtubule-dependence of the conversion (Fig. 3C and D) clearly indicated the involvement of compartments in the late stage of endocytosis. Furthermore, studies by others have demonstrated that the slow recycling compartments of Tf–TfR pathway merge with vesicles from the protein secretory route at the TGN [12,13]. Thus the TfR-mediated localization of endocytic ProINS-Tf might have enabled the contact of ProINS-Tf with a variety of endoproteases presented in secretory vesicles. Although we have not identified the enzyme(s) responsible for the conversion, it is conceivable that ProINS-Tf was processed by endoproteases belonging to the subtilisin-like prohormone convertase family. Predominantly localized in TGN, these convertases are considered responsible for the processing of proproteins routed to the secretory pathways [25,26].

In addition to the conversion, we also demonstrated that the generated irINS-Tf was biologically active and was reponsible for the observed long-term activities of ProINS-Tf. The short-term fusion protein treatments for either promotion of glucose uptake in adipocytes (Fig. 4) or a 5 min stimulation of Akt phosphorylation (Fig. 5A) were not sufficient for the conversion of ProINS-Tf to active irINS-Tf, and hence the activities primarily depended on the weak binding of ProINS moiety to IR. On the other hand, prolonged incubation of ProINS-Tf in H4IIE cells allowed adequate conversion to generate enough irINS-Tf to effectively elicit INS-related activities, both in stimulation of Akt phosphorylation (Fig. 5A and B) and inhibition of glucose production (Table 1). Furthermore, the decrease in conversion to irINS-Tf (Fig. 3A) correlated with the loss of the increased activity in inhibiting glucose production when excess apo-Tf was co-incubated with ProINS-Tf (Fig. 6). Taken together, these findings clearly demonstrated the TfR-mediated activation of ProINS-Tf as an inactive prodrug.

Many prodrug-activating strategies have been developed for protein drugs, such as exploiting specific environment at the target sites [27,28], co-delivering an activating molecule [29,30], or employing intracellular enzymes or proteases [31]. The intracellular activation strategy that utilizes the proteases in the protein secretory pathway has shown promise in the conversion of prohormones to hormones, e.g. the processing of ProINS [32,33]. However, a majority of these reported approaches are primarily limited to gene delivery and cellular expression methods. Results from our study suggest that, taking advantage of the Tf–TfR pathway, Tf-fusion protein approach can also employ the intracellular machinery to facilitate proprotein conversion and release, while circumventing the complex problems with gene delivery. Our conversion and activation results indicate that ProINS-Tf fusion protein may overcome problems encountered with ProINS, such as the ineffective *in vivo* conversion and requirement of high doses. The increased conversion efficiency, coupled with the advantages of the prolonged pharmacological half-life of Tf-fusion proteins [8,34], could potentially enable the use of ProINS-Tf in lower doses and thus reduce unwanted side-effects.

5. Conclusions

This is the first report describing the intracellular activation of proproteins using TfR-mediated endocytic and recycling mechanism. We demonstrated that ProINS-Tf fusion protein, with the aid of Tf–TfR binding, could be endocytosed into Tf slow recycling compartments, and converted to irINS-Tf that is subsequently released into the extracellular medium. Furthermore, we showed that the generated irINS-Tf was biologically active, and as a result, ProINS-Tf elicited TfR-mediated enhancement of activities in hepatoma cells. These findings imply the potential of using ProINS-Tf fusion protein as a prodrug for long-acting INS therapy and of exploiting Tf-fusion protein strategy as

a novel approach for the processing of proproteins to their biologically active counterparts.

Acknowledgements

We thank Robert H. Mo for the assistance in RIA experiments. The work was supported by NIH Grant GM063647. W.C.S. is John A. Biles Professor of Pharmaceutical Sciences.

References

[1] J.A. Galloway, S.A. Hooper, C.T. Spradlin, D.C. Howey, B.H. Frank, R.R. Bowsher, J.H. Anderson, Biosynthetic human proinsulin. Review of chemistry, in vitro and in vivo receptor binding, animal and human pharmacology studies, and clinical trial experience, Diabetes Care 15 (1992) 666–692.
[2] R.R. Revers, R. Henry, L. Schmeiser, O. Kolterman, R. Cohen, R. Bergenstal, K. Polonsky, J. Jaspan, A. Rubenstein, B. Frank, The effects of biosynthetic human proinsulin on carbohydrate metabolism, Diabetes 33 (1984) 762–770.
[3] R.M. Bergenstal, R.M. Cohen, E. Lever, K. Polonsky, J. Jaspan, P.M. Blix, R. Revers, J.M. Olefsky, O. Kolterman, K. Steiner, The metabolic effects of biosynthetic human proinsulin in individuals with type I diabetes, J. Clin. Endocrinol. Metab. 58 (1984) 973–979.
[4] H. Schatz, S. Ammermann, H. Laube, K. Federlin, Bioactivity and pharmacokinetics of human proinsulin in comparison to human insulin after intravenous and subcutaneous injection, Horm. Metab. Res. 20 (1988) 445–449.
[5] B.D. Given, R.M. Cohen, S.E. Shoelson, B.H. Frank, A.H. Rubenstein, H.S. Tager, Biochemical and clinical implications of proinsulin conversion intermediates, J. Clin. Invest. 76 (1985) 1398–1405.
[6] Y. Bai, D.K. Ann, W.C. Shen, Recombinant granulocyte colony-stimulating factor-transferrin fusion protein as an oral myelopoietic agent, Proc. Natl. Acad. Sci. U.S.A. 102 (2005) 7292–7296.
[7] N. Amet, W. Wang, W.C. Shen, Human growth hormone-transferrin fusion protein for oral delivery in hypophysectomized rats, J. Control. Release 141 (2010) 177–182.
[8] B.J. Kim, J. Zhou, B. Martin, O.D. Carlson, S. Maudsley, N.H. Greig, M.P. Mattson, E.E. Ladenheim, J. Wustner, A. Turner, H. Sadeghi, J.M. Egan, Transferrin fusion technology: a novel approach to prolonging biological half-life of insulinotropic peptides, J. Pharmacol. Exp. Ther. 334 (2010) 682–692.
[9] M.E. Brandsma, A.M. Jevnikar, S. Ma, Recombinant human transferrin: beyond iron binding and transport, Biotechnol. Adv. 29 (2011) 230–238.
[10] P.T. Gomme, K.B. McCann, J. Bertolini, Transferrin: structure, function and potential therapeutic actions, Drug Discov. Today 10 (2005) 267–273.
[11] A. Widera, F. Norouziyan, W.C. Shen, Mechanisms of TfR-mediated transcytosis and sorting in epithelial cells and applications toward drug delivery, Adv. Drug Deliv. Rev. 55 (2003) 1439–1466.
[12] W. Stoorvogel, H.J. Geuze, J.M. Griffith, G.J. Strous, The pathways of endocytosed transferrin and secretory protein are connected in the trans-Golgi reticulum, J. Cell Biol. 106 (1988) 1821–1829.
[13] J.B. Fishman, R.E. Fine, A trans Golgi-derived exocytic coated vesicle can contain both newly synthesized cholinesterase and internalized transferrin, Cell 48 (1987) 157–164.
[14] A.W. Harmon, D.S. Paul, Y.M. Patel, MEK inhibitors impair insulin-stimulated glucose uptake in 3T3-L1 adipocytes, Am. J. Physiol. Endocrinol. Metab. 287 (2004) E758–E766.
[15] M.F. White, The insulin signaling system and the IRS proteins, Diabetologia 40 (1997) S2–S17.
[16] M. Kitazawa, Y. Ohizumi, Y. Oike, T. Hishinuma, S. Hashimoto, Angiopoietin-related growth factor suppresses gluconeogenesis through the Akt/forkhead box class O1-dependent pathway in hepatocytes, J. Pharmacol. Exp. Ther. 323 (2007) 787–793.
[17] R.T. MacGillivray, S.A. Moore, J. Chen, B.F. Anderson, H. Baker, Y. Luo, M. Bewley, C.A. Smith, M.E. Murphy, Y. Wang, A.B. Mason, R.C. Woodworth, G.D. Brayer, E.N. Baker, Two high-resolution crystal structures of the recombinant N-lobe of human transferrin reveal a structural change implicated in iron release, Biochemistry 37 (1998) 7919–7928.
[18] A.B. Mason, Q.Y. He, P.J. Halbrooks, S.J. Everse, D.R. Gumerov, I.A. Kaltashov, V.C. Smith, J. Hewitt, R.T. MacGillivray, Differential effect of a his tag at the N- and C-termini: functional studies with recombinant human serum transferrin, Biochemistry 41 (2002) 9448–9454.
[19] J. Mather, P. Roberts, Introduction to cell and tissue culture, Plenum Press, New York, 1998.
[20] M.W. Greene, H. Sakaue, L. Wang, D.R. Alessi, R.A. Roth, Modulation of insulin-stimulated degradation of human insulin receptor substrate-1 by Serine 312 phosphorylation, J. Biol. Chem. 278 (2003) 8199–8211.
[21] P. Freychet, The interactions of proinsulin with insulin receptors on the plasma membrane of the liver, J. Clin. Invest. 54 (1974) 1020–1031.
[22] V. Jurisic, T. Srdic-Rajic, G. Konjevic, G. Bogdanovic, M. Colic, TNF-alpha induced apoptosis is accompanied with rapid CD30 and slower CD45 shedding from K-562 cells, J. Membr. Biol. 239 (2011) 115–122.
[23] V. Jurisic, I. Spuzic, G. Konjevic, A comparison of the NK cell cytotoxicity with effects of TNF-alpha against K-562 cells, determined by LDH release assay, Cancer Lett. 138 (1999) 67–72.
[24] S. Mukherjee, R.N. Ghosh, F.R. Maxfield, Endocytosis, Physiol. Rev. 77 (1997) 759–803.
[25] A. Zhou, G. Webb, X. Zhu, D.F. Steiner, Proteolytic processing in the secretory pathway, J. Biol. Chem. 274 (1999) 20745–20748.
[26] S.P. Smeekens, Processing of protein precursors by a novel family of subtilisin-related mammalian endoproteases, Biotechnol. (N Y) 11 (1993) 182–186.
[27] I. Watermann, J. Gerspach, M. Lehne, J. Seufert, B. Schneider, K. Pfizenmaier, H. Wajant, Activation of CD95L fusion protein prodrugs by tumor-associated proteases, Cell Death Differ. 14 (2007) 765–774.
[28] M. Inoue, M. Mukai, Y. Hamanaka, M. Tatsuta, M. Hiraoka, S. Kizaka-Kondoh, Targeting hypoxic cancer cells with a protein prodrug is effective in experimental malignant ascites, Int. J. Oncol. 25 (2004) 713–720.
[29] J.F. Liang, Y.J. Park, H. Song, Y.T. Li, V.C. Yang, ATTEMPTS: a heparin/protamine-based prodrug approach for delivery of thrombolytic drugs, J. Control. Release 72 (2001) 145–156.
[30] H. Wang, H. Song, V.C. Yang, A recombinant prodrug type approach for triggered delivery of streptokinase, J. Control. Release 59 (1999) 119–122.
[31] V.M. Rivera, X. Wang, S. Wardwell, N.L. Courage, A. Volchuk, T. Keenan, D.A. Holt, M. Gilman, L. Orci, F. Cerasoli Jr., J.E. Rothman, T. Clackson, Regulation of protein secretion through controlled aggregation in the endoplasmic reticulum, Science 287 (2000) 826–830.
[32] C. Arcelloni, L. Falqui, S. Martinenghi, A. Stabilini, A.E. Pontiroli, R. Paroni, Processing and release of human proinsulin-cleavage products into culture media by different engineered non-endocrine cells: a specific assessment by capillary electrophoresis, J. Endocrinol. 166 (2000) 437–445.
[33] A.M. Abai, P.M. Hobart, K.M. Barnhart, Insulin delivery with plasmid DNA, Hum. Gene Ther. 10 (1999) 2637–2649.
[34] X. Chen, H.F. Lee, J.L. Zaro, W.C. Shen, Effects of Receptor Binding on Plasma Half-Life of Bifunctional Transferrin Fusion Proteins, Mol. Pharm. 8 (2011) 457–465.